VI International Conference on Computational Methods for Coupled Problems in Science and Engineering
COUPLED PROBLEMS 2015
B. Schrefler, E. Oñate and M. Papadrakakis (Eds)

NUMERICAL SIMULATION OF FLOW INTERACTION BETWEEN STATIONARY AND DOWNSTREAM ELASTICALLY MOUNTED CYLINDERS AT LOW REYNOLDS NUMBERS

PAULO R. F. TEIXEIRA[*] AND ERIC DIDIER[†]

[*] Universidade Federal do Rio Grande (FURG)
Avenida Itália km8, Campus Carreiros, 96203-900, Rio Grande, RS, Brazil
E-mail address: pauloteixeira@furg.br; web page: http://www.furg.br

[†] Departamento de Hidráulica e Ambiente, Laboratório Nacional de Engenharia Civil (LNEC)
Avenida do Brasil, 101, 1700-066, Lisbon, Portugal
E-mail address: edidier@lnec.pt; web page: http://www.lnec.pt

Key words: Finite Element Method, Flow-induced Vibration, Circular Cylinders, Tandem Arrangement, Wake Interference.

Abstract. The vortex-induced vibration phenomenon can occur as a result of the action of wind on bridges, slender buildings, chimneys and energy transmission cables besides the action of water flow on pipelines and risers, among others. Despite the simplicity of the geometry of the circular cylinders, the uniform flow around them is very complex and important, since it may induce unsteady forces on structures associated with vortex shedding. This paper describes the study of two circular cylinders in tandem arrangement subject to bi-dimensional uniform laminar flows at low Reynolds numbers. The numerical model Ifeinco, which is based on the finite element method and uses a partitioned scheme that considers two-way interaction of fluid flow and structure, has been employed in the analysis. The fluid flow model uses a semi-implicit two-step Taylor-Galerkin method to discretize the Navier-Stokes equations whereas the arbitrary Lagrangean-Eulerian formulation to follow the cylinder motion. This movement has been described by the one DOF dynamic equation for the transverse direction discretized in time by the implicit Newmark method. Both cylinders are immersed in water and the downstream one is elastically mounted in transversal direction. Firstly, stationary cylinders in tandem arrangement for Re = 100 are analysed for L/D from 1.5 to 6.0. Results of lift and drag coefficients and Strouhal number are compared with other numerical results and good agreement is found. These analyses show that the vortex shedding occurs for both cylinders for gaps $L/D > 4.0$ and the wake behind the downstream cylinder is formed by the combination of vortex shed of both cylinders. Secondly, numerical simulations considering downstream elastically mounted cylinder for $L/D = 5.25$ are analysed for Reynolds numbers ranging from 100 to 140. It shows that the resonance occurred for Reynolds numbers between 115 and 120, unlike the range obtained for a single cylinder, from 102 to 113, submitted to the same conditions. Furthermore, the maximum dimensionless amplitude of oscillation is 0.721 for Re = 118, which is much higher than the one of the single cylinder (0.422 for Re = 103). The interaction between cylinders changes the Strouhal number in relation to the one of the single cylinder; because of this, there are differences between the lock-in regions.

1 INTRODUCTION

The vortex-induced vibration phenomenon can occur as a result of the action of wind on bridges, slender buildings, chimneys and energy transmission cables besides the action of water flow on pipelines and risers. The wake around circular cylinders due to a uniform flow leads to several complex phenomena. Despite the simplicity of geometry, the flow around cylinders requires deep studies, since it may induce unsteady forces on structures associated with vortex shedding.

This phenomenon, which appears in many practical situations of different bluff body arrangements, has its complexity increased due to the wake interference among circular cylinders. Several interference regimes have been classified, according to the Reynolds number and distance between cylinders, based on experimental studies, such as Igarashi's [1], Zdravkovich's [2,3] and Sumner et al.'s [4]. Considering tandem arrangement of circular cylinders [1,5], a critical distance, Lc, between both cylinders is identified ($L/D \approx 4$, where L is the center to center distance between cylinders and D is the diameter) in which discontinuity of the flow behavior and vortex shedding occur. For shorter distances ($L < Lc$), the mean drag of the downstream cylinder is small and negative. For longer distances ($L > Lc$), fluctuating lift and drag forces of the downstream cylinder become higher than the upstream ones.

Researchers, such as Zdravkovich [6], Brika and Laneville [7], investigated experimentally the flow induced oscillations of two interfering circular cylinders considering different arrangements and distances between them. The authors observed that the vortex induced oscillations are strongly dependent on the arrangement of cylinders and the gap between cylinders. Assi et al. [8], Okajima et al. [9] and Huera-Huarte and Gharib [10] analyzed experimentally the flow induced oscillations specifically for tandem arrangements.

Other researchers, such as Li et al. [11], Slaouti and Stanby [12], Mittal et al. [13], Meneghini et al. [14], Sharman et al. [15], Carmo [16], Carmo and Meneghini [17], studied several parameters of the flow for different arrangements between cylinders based on numerical simulations. Some numerical analyses (Carmo et al. [18], Mittal and Kumar [19], Papaioannou et al. [20]) have been developed for the study of fluid-structure interaction in tandem arrangements of circular cylinders considering two-dimensional cases at different Reynolds numbers, by using vortex discrete method, finite volume method and spectral element method.

This paper describes the study of two circular cylinders in tandem arrangement subject to bi-dimensional uniform laminar flows at low Reynolds numbers (from 90 to 140). Firstly, stationary cylinders in tandem arrangement for Re = 100 are analysed for L/D from 1.5 to 6.0. Afterwards, cases with center to center distance between cylinders equal to $5.25D$ for both fixed cylinders and for fixed upstream cylinder and a downstream one elastically mounted in transversal direction are analysed. The numerical model Ifeinco [21] which is based on the finite element method and uses a partitioned scheme that considers two-way interaction of fluid flow and structure is employed for the analysis.

2 IFEINCO MODEL

The numerical model Ifeinco is based on a partitioned scheme, in which the fluid flow and

the structure are solved in two-way interaction. Basically, updating the variables of the flow consists of following steps [22]:

a) Calculate non-corrected momentum per volume $\tilde{U}_i$ at $t+\Delta t/2$, where the pressure term is at t instant, according to Eq. (1).

$$\tilde{U}_i^{n+1/2} = U_i^n - \frac{\Delta t}{2}\left(\frac{\partial f_{ij}^n}{\partial x_j} - \frac{\partial \tau_{ij}^n}{\partial x_j} + \frac{\partial p^n}{\partial x_i} - w_j^n \frac{\partial U_i^n}{\partial x_i}\right) \tag{1}$$

where p is the pressure, w_i are the velocity components of the reference system, τ_{ij} is the viscous stress tensor, $U_i = \rho \mathrm{v}_i$, $f_{ij} = \mathrm{v}_j(\rho \mathrm{v}_i) = \mathrm{v}_j U_i$ $(i, j = 1, 2)$, ρ is the specific mass and v_i are the velocity components.

b) Update the pressure p at $t+\Delta t$, given by the Poisson equation:

$$\frac{1}{c^2}\Delta p = -\Delta t\left[\frac{\partial \tilde{U}_i^{n+1/2}}{\partial x_i} - \frac{\Delta t}{4}\frac{\partial}{\partial x_i}\frac{\partial \Delta p}{\partial x_i}\right] \tag{2}$$

where $\Delta p = p^{n+1} - p^n$ and $i = 1, 2$.

c) Correct the velocity at $t+\Delta t/2$, adding the pressure variation term from t to $t+\Delta t/2$, according to the equation:

$$U_i^{n+1/2} = \tilde{U}_i^{n+1/2} - \frac{\Delta t}{4}\frac{\partial \Delta p}{\partial x_i} \tag{3}$$

d) Calculate the velocity at $t+\Delta t$ using variables updated in the previous steps as follows:

$$U_i^{n+1} = U_i^n - \Delta t\left(\frac{\partial f_{ij}^{n+1/2}}{\partial x_j} - \frac{\partial \tau_{ij}^{n+1/2}}{\partial x_j} + \frac{\partial p^{n+1/2}}{\partial x_i} - w_j^{n+1/2}\frac{\partial U_i^{n+1/2}}{\partial x_i}\right) \tag{4}$$

The classical Galerkin weighted residual method is applied to the space discretization of Eq. (1), (2), (3) and (4), and a triangular element is employed. In the variables at $t+\Delta t/2$ instant, a constant shape function is used, and in the variables at t and $t+\Delta t$, a linear shape function is employed [21].

The Poisson equation, which is a result of spatial discretization of Eq. (2), is solved by employing the conjugate gradient method with a diagonal preconditioning [23]. Spatially discretized Equation (4) is explicitly solved by the iterative process using the lumped matrix [24].

The mesh velocity transversal component w_2 is computed to diminish element distortions, keeping prescribed velocities on moving and stationary boundary surfaces. The mesh movement algorithm adopted in this paper uses a smoothing procedure for the velocities based on these boundary lines [21].

In order to update the rigid body motion of the structure, it is necessary to calculate displacements and rotations of a hypothetical concentrated mass at its gravity center. In this case study, there is only movement in transverse direction (one degree of freedom – DOF) and, consequently, displacement, velocity and acceleration in this direction are the variables to be determined at each time step. To update the variables of the structure, the rigid motion

of the cylinder is calculated at each instant, after the variables of the flow (pressure and viscous stress) are known. For this case study, one DOF dynamic equation is considered for the transverse direction, as follows:

$$m\ddot{y} + c\dot{y} + ky = F \tag{8}$$

where $\ddot{y}$, $\dot{y}$ and y are the transverse acceleration, velocity and displacement, respectively; m is the mass; c is the damping coefficient; k is the stiffness; and F is the dynamic force. In Ifeinco code, Eq. (8) is discretized in time by using the implicit Newmark method [25].

3 NUMERICAL SIMULATION

Both cylinders, which are immersed in water, have diameters D = 0.0016 m and their center to center distance between cylinder is equal to L (Fig. 1). In cases when the downstream cylinder (mass m = 0.2979 kg) is considered elastically mounted in transversal direction, the spring stiffness, k, is equal to 579 N/m, resulting in a natural frequency of f_n = 7.016 Hz while the damping coefficient, c, is equal to 0.0325 kg/s, its correspondent damper ratio is $\zeta = c / 2m\omega_n$ = 0.0012, where ω_n is the angular frequency, and the mass ratio ($M = m/\rho D^2$, where ρ is the specific mass of fluid) is equal to 166 [26]. Constant velocity (U_∞) is imposed on the inlet boundary whereas, on the lateral boundaries (far from cylinders), a slide condition is imposed; the outlet boundary is free exit, but null pressure is imposed on its center.

The computational domain consists of a rectangle whose sides have the minimum distance from the cylinders of 100D. The cylinder boundary is discretized in 200 segments and the size of the first element around the cylinders is 0.016D, totalizing from 228000 to 252000 nodes and from 455000 to 505000 triangular elements, depending on the distance between both cylinders. The time step is between $6\text{x}10^{-5}$ s and $8.5\text{x}10^{-5}$ s, according to the Reynolds number [27].

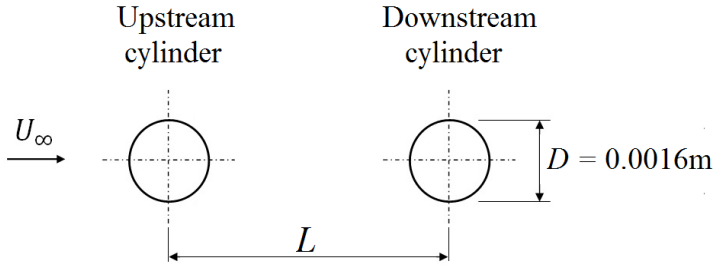

Figure 1: Sketch of the case study

3.1 Stationary upstream and downstream cylinders

In this section, stationary cylinders in tandem arrangement for Reynolds number, Re, equal to 100 (Re = $\rho U_\infty D/\mu$, where μ is the viscosity) are analysed for L/D from 1.5 to 6.0. Results are compared with other numerical ones presented by Didier [5] and Sharman et al. [15].

Figure 2 shows Strouhal numbers ($St = f D/U_\infty$, where f is the vortex shedding frequency) for L/D from 1.5 to 6.0. Ifeinco results had good agreement with those obtained by other authors. Figure 2 indicates the strong influence of the cylinder distances on the Strouhal

number, which experiments an abrupt variation at *L/D* around 4.0 and increases almost 30% from *L/D* = 3.5 to 4.0. The Strouhal numbers are lower than 0.1641, which is the value obtained by Ifeinco for a single cylinder, but the more the distance between both cylinders increases (diminishing the interference between them), the closer the Strouhal number gets to that value.

The distance between cylinders of 4.0 *D*, in which an abrupt variation in the Strouhal number occurs, is named the critical spacing (*Lc*). Different flow behaviors are observed when cases with distances shorter and longer than *Lc* are compared. The analysis of the streamlines for *L/D* = 2.0 (*L* < *Lc*) and 4.0 (*L* > *Lc*), shown in Fig. 5, explains these differences. For *L/D* = 2.0, the wake off the upstream cylinder reattaches to the downstream one and a symmetrical flow pattern occurs between both cylinders. Moreover, long vortices are shed off the downstream cylinder, a fact that results in the lower Strouhal number. For *L/D* = 4.0, vortices are also shed off the upstream cylinder; it moves the reattachment point and energizes the fluid that flows completely around the downstream cylinder.

Figures 3 and 4 show the root mean square lift (C_{Lrms}) and the mean drag (C_{Dmean}) coefficients for different cylinder distances, respectively. The critical spacing (*Lc*) is clear in both figures and the lower values of C_{Lrms} and C_{Dmean} before *Lc* have been explained by the flow behavior shown in Fig. 5. Cases in which *L* > *Lc*, the interference between cylinders provides values of C_{Lrms} higher than those obtained by Ifeinco for the single cylinder (0.2268), considering the same Reynolds number. It occurs with more intensity for the downstream cylinder that is subject to the shed of the upstream one. Figure 4 shows that the mean drag of downstream cylinder is negative for smaller spacing, i.e., this cylinder is pushed forwards by the fluids. From that moment on, the more the distance between both cylinders increases, the more the mean drag slowly increases to small positive values and then varies abruptly at critical spacing. The upstream cylinder presents higher values of C_{Dmean} by comparison with downstream cylinder one, but lower than that obtained by Ifeinco for single cylinder (1.3208).

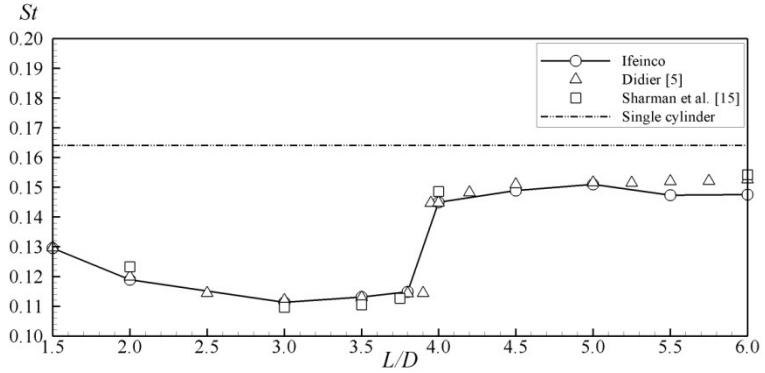

Figure 2: Strouhal number versus *L/D* for stationary cylinder cases.

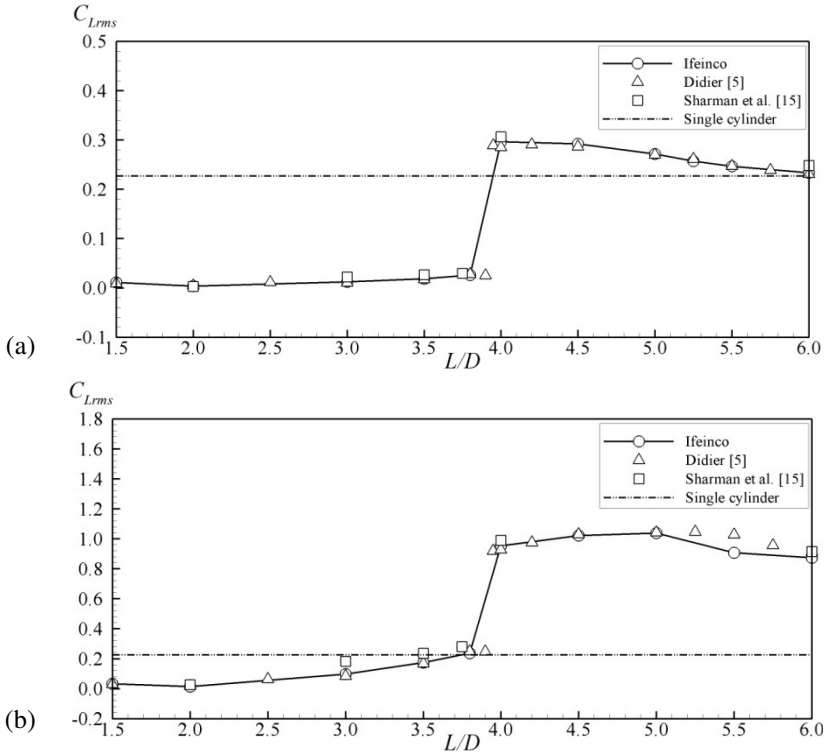

Figure 3: Root mean square of lift coefficient versus *L/D* for upstream cylinder (a) and downstream one (b) in stationary cylinder cases.

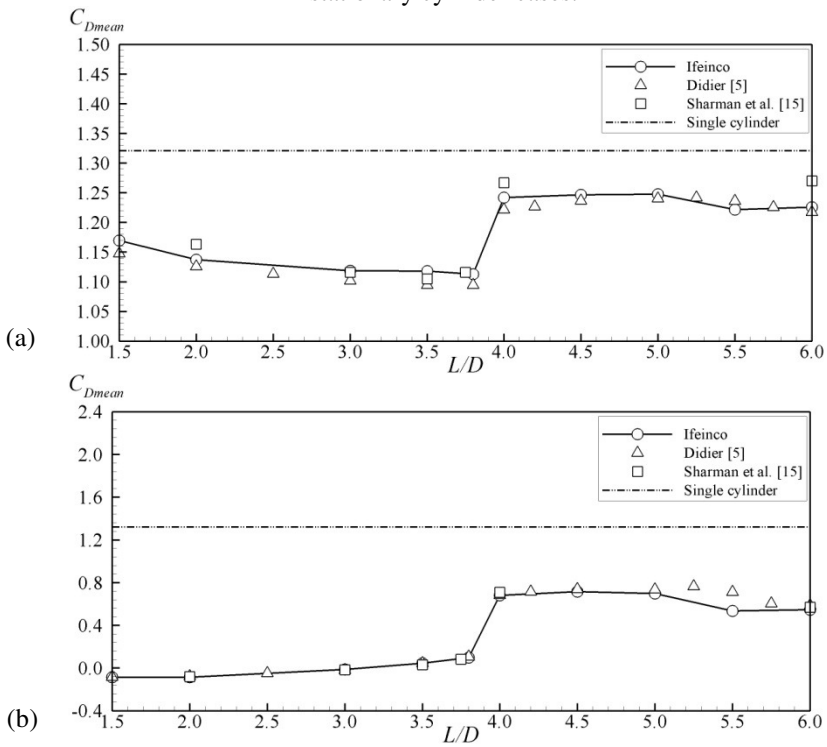

Figure 4: Mean drag coefficient versus *L/D* for upstream cylinder (a) and downstream one (b) in stationary cylinder cases.

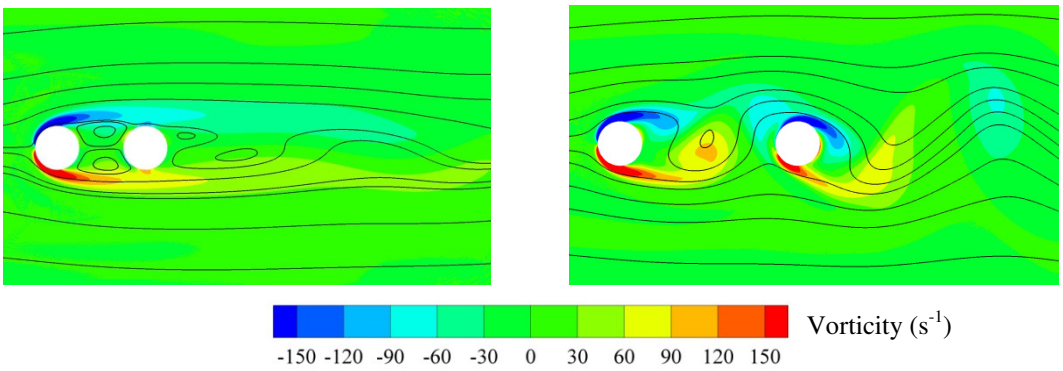

Figure 5: Streamlines around the stationary cylinders for L/D = 2.0 (a) and 4.0 (b).

3.2 Stationary upstream and oscillating downstream cylinders

In this section, the center to center distance between cylinders is 5.25D, the downstream cylinder is elastically mounted and the analysis is performed for Reynolds numbers ranging between 90 and 140, thus, characterizing a regime in which the vortex street is fully laminar and bi-dimensional. Therefore, vortices are expected to shed off the upstream cylinder and roll up before striking the downstream cylinder, thus, strongly interacting with it. For L/D = 5.25, an interesting maximum occurs in C_{Lrms} due to the synchronization of vortex shedding: vortices shed from the upstream cylinder add to the vortices shed from the downstream one, in a way that the fluctuating lift force reaches its maximum. The main dimensionless parameter that influences the VIV behavior is the reduced velocity ($V_R = U_\infty/D\,f_n$), ranging from 5 to 7.8 in this case.

In this case, a significant increase in C_{Lrms} from 1.001 to 1.701 at Reynolds number from 110 (V_R = 6.12) to 119 (V_R = 6.63) and an abrupt decrease in 0.687 at Re = 120 (V_R = 6.68) are observed. This phenomenon is characteristic of the resonance (lock-in) and also occurs in the single cylinder, but with some differences in coefficient magnitude and Reynolds number range, as shown in Fig. 6. The Reynolds number range in which this phenomenon occurs for single cylinder is wider than the range in the tandem arrangement case. Besides, in these regions, the mean drag coefficient for oscillating cylinder gets higher values abruptly, reaching 0.85 for Reynolds number of 117 (V_R = 6.51), as shown in Fig. 7. Similar behavior occurs in the single cylinder case, but with a wider Reynolds number range.

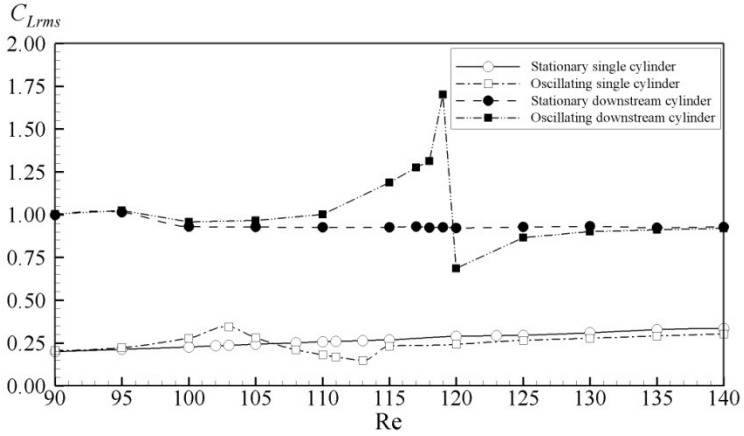

Figure 6: Root mean square of the lift coefficient versus Reynolds number for stationary and oscillating downstream cylinders in tandem arrangement and for fixed and oscillating single cylinders

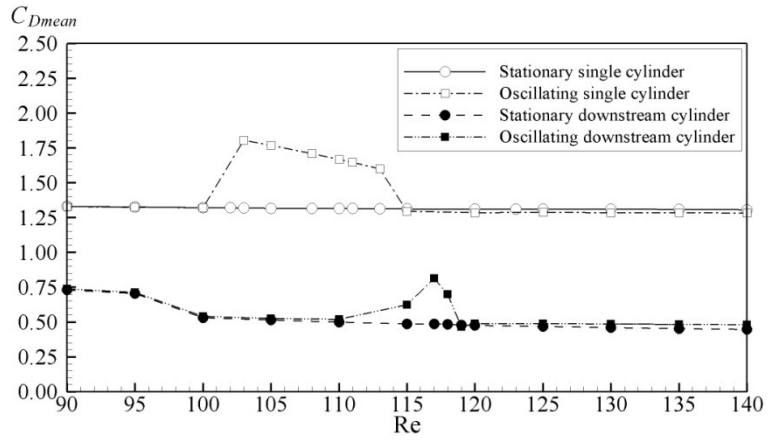

Figure 7: Mean drag coefficient versus Reynolds number for stationary and oscillating downstream cylinders in tandem arrangement and for fixed and oscillating single cylinders

Figure 8 shows the root mean square of lift coefficient and the mean drag coefficient versus Reynolds number for stationary upstream and oscillating downstream cylinders. It may be noticed that while the downstream cylinder experiments high variations of coefficients in the lock-in region, these coefficients decrease smoothly for the upstream cylinder. In this case, flow interference between both cylinders is different from the stationary downstream cylinder due to the motion of the downstream cylinder and changes in wake pattern and pressure field.

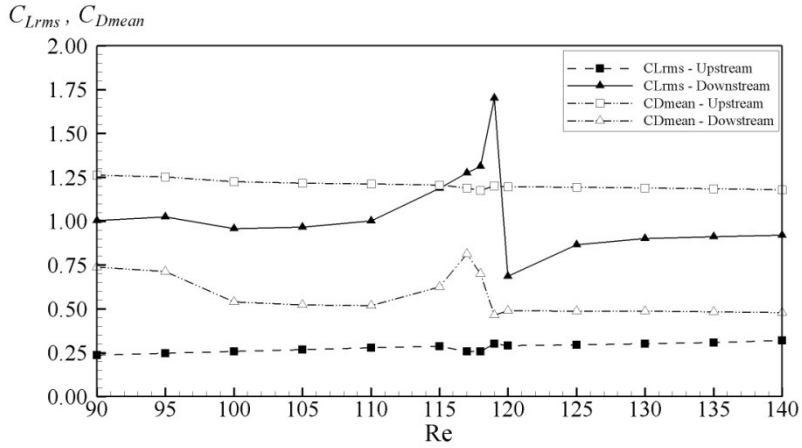

Figure 8: Root mean square of lift and mean drag coefficients versus Reynolds number for stationary upstream and oscillating downstream cylinders in tandem arrangement

Figure 9 shows the dimensionless amplitude (Y/D) and the vortex induced vibration frequency (f/f_n) for downstream cylinder and a comparison with the single one. It can be noticed that the resonance, for the single cylinder, occurred for Reynolds numbers between 102 (V_R = 5.68) and 113 (V_R = 6.29) case in which the vibration amplitude is higher and the vortex frequency is approximately equal to the natural frequency (f_n) of the dynamic system. In tandem arrangement with L/D = 5.25, the downstream cylinder experiments the resonance

in a shorter Reynolds number range, between 115 (V_R = 6.40) and 120 (V_R = 6.68). Furthermore, the maximum dimensionless amplitude is 0.721 for Re = 118 and this is much higher (more than 70%) than the one for the single cylinder (0.422 for Re = 103). The interference effects on tandem arrangement change the Strouhal number in relation to the single cylinder one and to the mode of interference between both cylinders, since the downstream cylinder is immersed in the periodic wake of the upstream one. This is why there are differences between both lock-in regions.

Figure 10 shows the temporal series of lift coefficient (C_L) and dimensionless vibration amplitude (Y/D) for Re = 118. Vorticity distributions and streamlines are shown in Fig. 11 where time positions of each picture are indicated in Fig. 10. It may be noticed that the lift coefficient presents higher non linearity by comparison with vibration amplitude which shows harmonic behavior. The phase angle between them is around 42° in this case. Figure 10 shows that the vortex shedding occurs for both cylinders, as expected for $L/D > 4$, and the wake behind the downstream cylinder is formed by the combination of vortex shed from both cylinders. The maximum vibration amplitude (Y/D = 0.721) occurs at instants shown in Fig. 11a and 11b.

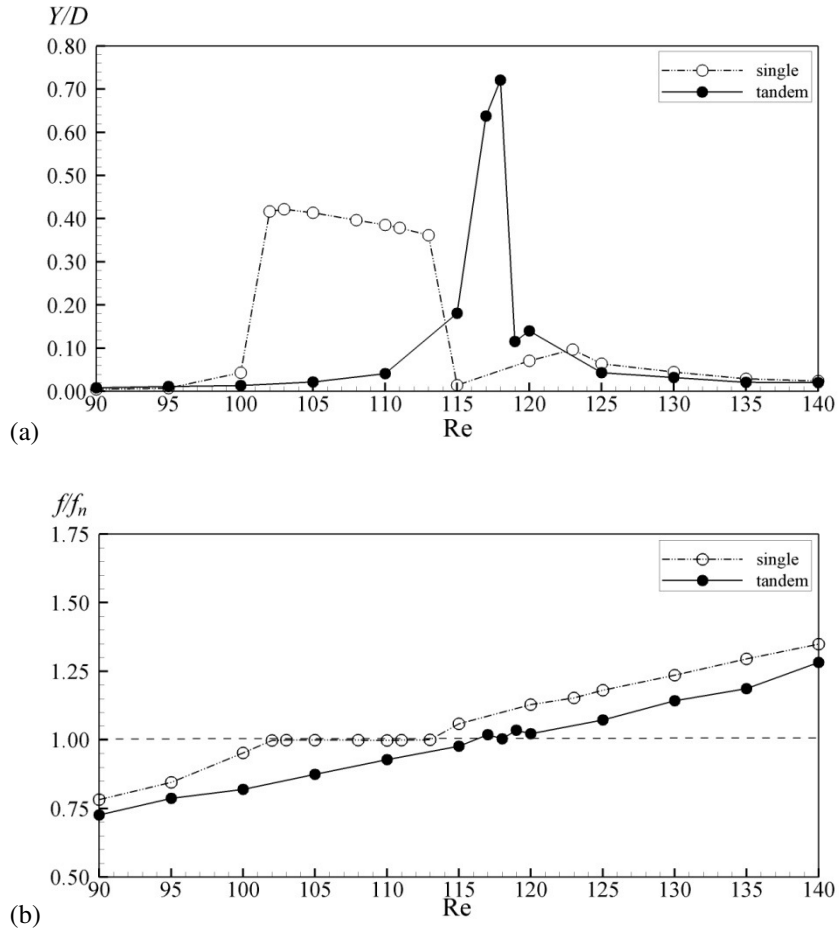

Figure 9: Dimensionless vibration amplitude (Y/D) (a) and vortex shedding frequency (f/f_n) (b) versus Reynolds numbers for single cylinder and cylinders in tandem arrangement

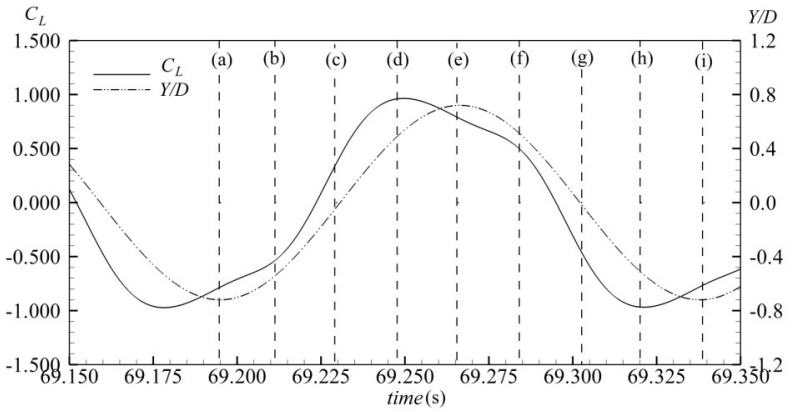

Figure 10: Temporal series of lift coefficient (C_L) and dimensionless vibration amplitude (Y/D) for Re = 118 (letters represent time positions of the vorticity distributions, shown in Fig. 10)

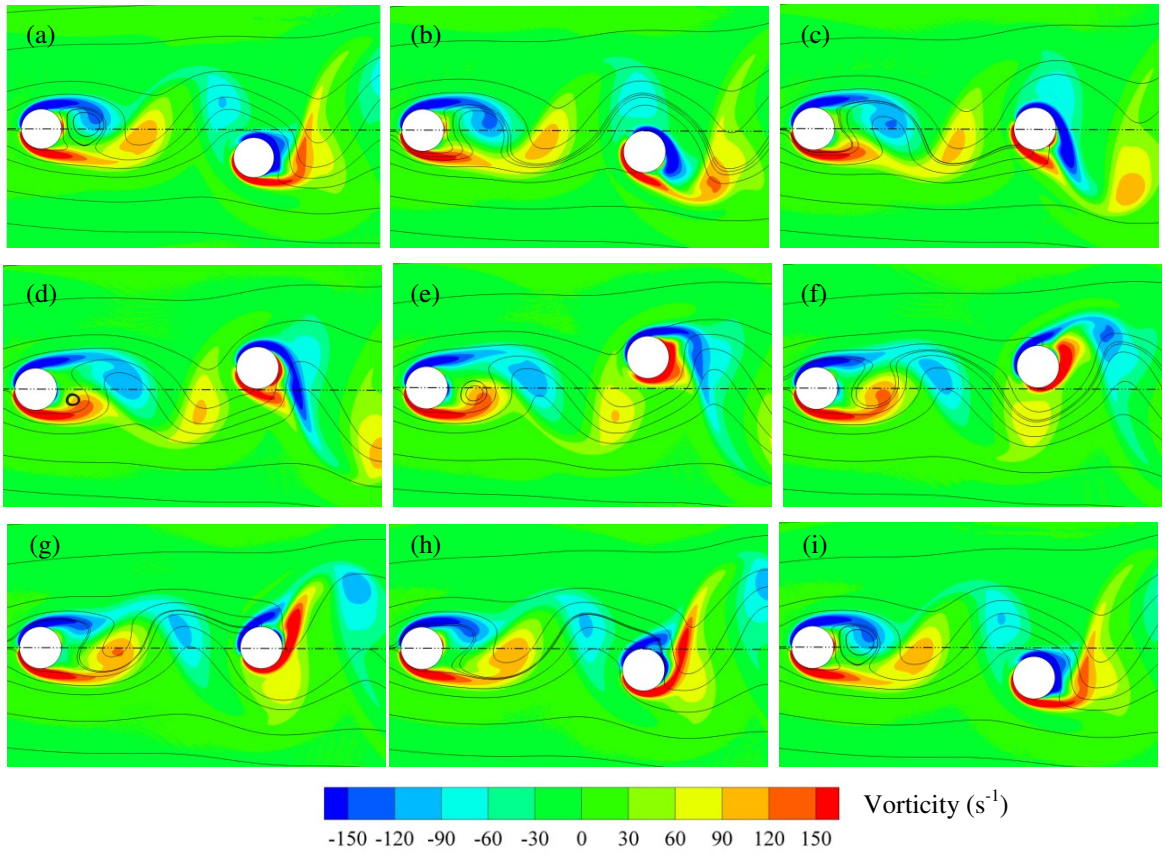

Figure 11: Vorticity and streamlines around cylinders for Re = 118 at nine instants (shown in the graph in Fig. 9) during one cycle

4 CONCLUSION

This paper presented a numerical analysis of a uniform flow over circular cylinders in tandem arrangement at low Reynolds numbers. Simulations were carried out by using Ifeinco

model which is based on the finite element method and employs the semi-implicit two-step Taylor-Galerkin method to discretize the Navier-Stokes equations and the Newmark method for the dynamic equation of the structure.

Ifeinco results (Strouhal number, root mean square lift and mean drag coefficients) had good agreement with those obtained by other authors for stationary cylinders, *L*/*D* from 1.5 to 6.0 and Re = 100. The critical spacing (*Lc*) equal to 4.0 *D* was obtained and abrupt variations in the flow parameters were observed in this case. Different flow behaviors were noticed when distances were shorter and longer than *Lc*. For $L < Lc$, vortices wake off the upstream cylinder and reattach to the downstream one while a symmetrical flow pattern occurs between both cylinders. For $L > Lc$, vortices shed off both cylinders.

Considering the center to center distance equal to 5.25*D* and the downstream cylinder elastically mounted in transversal direction, the lock-in region was captured by Reynolds number from 115 to 120; this range was different from and shorter than the one for the single cylinder (102 to 113). The maximum vibration amplitude, which was 0.721*D*, was higher than the one for the single cylinder (0.422*D*). At Re = 120 (in the lock-in region), the drag coefficient and the lift coefficient showed abrupt variations; the latter was much more intense. Complex interference occurs between both cylinders since the downstream cylinder is immersed in the periodic wake of the upstream one.

REFERENCES

[1] Igarashi, T. Characteristics of the flow around two circular cylinders arranged in tandem. *Bulletin of JSME* (1977) **24**(188):323-331.

[2] Zdravkovich, M.M. Review of flow interference between two circular cylinders in various arrangements. *ASME Journal of Fluids Engineering* (1977) **99**:618-633.

[3] Zdravkovich, M.M. The effects of interference between circular cylinders in cross flow. *Journal of Fluids and Structures* (1987) **1**:618-633.

[4] Sumner, D., Price, S.J. and Païdoussis, M.P. Flow-pattern identification for two-staggered circular cylinders in cross-flow. *Journal of Fluid Mechanics* (2000) **411**:263-303.

[5] Didier, E. Numerical simulation of low Reynolds number flows over two circular cylinders in tandem. *Conference on Modelling Fluid Flow*, Budapest, September 9-12, (2009) 347-354.

[6] Zdravkovich, M.M. Flow induced oscillations of two interfering circular cylinders. *Journal of Sound and Vibration* (1985) **101**(4):511-521.

[7] Brika, D. and Laneville, A. The flow interaction between a stationary cylinder and a downstream flexible cylinder. *Journal of Fluids and Structures* (1999) **13**:579-606.

[8] Assi, G.R.S., Meneghini, J.R., Aranha. J.A.P., Bearman, P.W. and Casaprima, E. Experimental investigation of flow-induced vibration interference between two circular cylinders. *Journal of Fluids and Structures* (2006) **22**: 819:827.

[9] Okajima, A., Yasui, A., Kiwata, T. and Kimura, S. Flow-induced treamwise oscillation of two circular cylinders in tandem arrangement. *International Journal of Heat and Fluid Flow* (2007) **28**:552-560.

[10] Huera-Huarte, F.J. and Gharib, M. Vortex- and wake-induced vibrations of a tandem arrangement of two flexible circular cylinders with far wake interference. *Journal of*

Fluids and Structures (2011) **27**:824-828.
[11] Li, J., Chambarel, A., Donneaud, M. and Martin, R. Numerical study of laminar flow past one and two circular cylinders. *Computers & Fluids* (1991) **19**:155-170.
[12] Slaouti, A. and Stanby, P.K. Flow around two circular cylinders by the random-vortex method. *Journal of Fluids and Structures* (1992) **6**:641-670.
[13] Mittal, S., Kumar, V. and Raghuvanshi A. Unsteady incompressible flows past two cylinders in tandem and staggered arrangements. *International Journal for Numerical Methods in Fluids* (1997) **25**:1315-1344.
[14] Meneghini, J.R., Saltara, F., Siqueira, C.L. and Ferrari, J.A. Numerical simulation of flow interference between two circular cylinders in tandem and side by side arrangements. *Journal of Fluids and Structures* (2001) **15**:327-350.
[15] Sharman, B.. Lien, F.S., Davidson, L. And Norberg, C. Numerical predicitions of low Reynolds number flows over two tandem circular cylinders. *International Journal for Numerical Methods in Fluids* (2005) **47**:423-447.
[16] Carmo, B.S. Estudo numérico do escoamento ao redor de cilindros alinhados. Master Thesis, Escola Politécnica da Universidade de São Paulo (2005).
[17] Carmo, B.S. and Meneghini, J.R. Numerical investigation of the flow around two circular cylinders in tandem. *Journal of Fluids and Structures* (2006) **22**:979-988.
[18] Carmo, B.S., Sherwin, S.J., Bearman, P.W. and Willden, R.H.J. Flow-induced vibration of a circular cylinder subjected to wake intereference at low Reynolds number. *Journal of Fluids and Structures* (2011) **27**:503-522.
[19] Mittal, S. and Kumar, V. Flow-induced oscillations of two cylinders in tandem and staggered arrangements. *Journal of Fluids and Structures* (2001) **15:**717-736.
[20] Papaioannou, G.V., Yue, D.K.P., Triantafyllou, M.S. and Karniadakis, G.E. On the effect of spacing on the vortex-induced vibrations of two tandem cylinders. *Journal of Fluids and Structures* (2008) **24**:833-854.
[21] Teixeira, P.R.F. and Awruch, A.M. Numerical simulation of fluid-structure interaction using the finite element method. *Computers & Fluids* (2005) **34**:249–273.
[22] Teixeira, P.R.F. and Awruch, A.M. Three–dimensional simulation of high compressible flows using a multi-time-step integration technique with subcycles. *Applied Mathematical Modelling* (2001) **25**:613–627.
[23] Argyris, J., Doltsinis, J.St., Wuestenberg, H. and Pimenta, P.M. *Finite element solution of viscous flow problems*. Finite Elements in Fluids. Wiley, New York, Vol. 6, 89–114, (1985).
[24] Donea J., Giuliani, S., Laval and H., Quartapelle, L. Finite element solution of the unsteady Navier-Stokes equations by a fractional step method. *Computer Methods in Applied Mechanics and Engineering* (1982) **33**:53–73.
[25] Bathe, K.J. *Finite element procedures*. Prentice-Hall, (1996).
[26] Fredsϕe, J. and Sumer, B.M. *Hydrodynamics around cylindrical structures*. World Scientific Publishing Co. Pte. Ltd., Singapore, Vol. 12, (1997).
[27] Gonçalves, R.A., Teixeira P.R.F. and Didier, E. Numerical simulations of low Reynolds number flows past elastically mounted cylinder. *Thermal Engineering* (2012) **11**(1-2):61-67.